

Electric field and substrate effects dominate spin-phonon relaxation in graphene

Adela Habib,^{1,*} Junqing Xu,^{2,*} Yuan Ping,^{2,†} and Ravishankar Sundararaman^{1,3,‡}

¹*Department of Physics, Applied Physics and Astronomy, Rensselaer Polytechnic Institute, Troy, NY 12180, USA*

²*Department of Chemistry and Biochemistry, University of California, Santa Cruz, CA 95064, USA*

³*Department of Materials Science and Engineering, Rensselaer Polytechnic Institute, Troy, NY 12180, USA*

(Dated: September 14, 2022)

Experimental spin relaxation times in graphene, critical for spintronics and quantum information technologies, are two orders of magnitude below previous theoretical predictions for spin-phonon relaxation. Here, *ab initio* density-matrix dynamics simulations reveal that electric fields and substrates strongly reduce spin-phonon relaxation time to the nanosecond scale, in agreement with experiments. Our predicted out-of-plane to in-plane lifetime ratio exceeds 1/2 on boron nitride substrates, matching experiment unlike previous models, suggesting that spin-phonon relaxation is dominant in graphene at room temperature.

Graphene is a promising material platform for spintronics and spin-qubits in quantum information applications because of the potential for long-lived spin states, with predicted intrinsic limits due to spin-phonon relaxation at the microsecond scale.^{1–3} However, experimental measurements typically find lifetimes at the nanosecond scale, at least two orders of magnitude below the predicted intrinsic limit.^{4–11} Additionally, theoretical studies predict the out-of-plane to in-plane spin lifetime ratio to be exactly 1/2, stemming from a fully in-plane spin-orbit (SO) field.^{12,13} In contrast, measured values for this spin-relaxation anisotropy ratio strongly exceed 1/2 with typical values from 0.7 to 1.1.^{10,11,14,15} These two discrepancies underpin an ongoing debate about which spin relaxation mechanism dominates in graphene-based devices.¹⁶

Theoretical studies based on model Hamiltonians have investigated the role of flexural phonons, charged impurities and substrate-induced corrugations, and find these effects to be insufficient to explain the two order-of-magnitude discrepancy in spin lifetimes.^{12,13,17} Other studies propose extrinsic sources to play a major role, including electron-hole puddle relaxation dynamics,¹⁸ coupled interaction of spin and pseudospin in the presence of adatoms,¹⁹ and resonant magnetic impurities from polymer residues.²⁰ Further, previous models attribute the disagreement in the anisotropy ratio to extrinsic modifications to the effective SO magnetic field, such as from a substrate. However, such models cannot directly predict the magnitudes of these effective fields, and hence cannot establish this explanation unambiguously.

In this Letter, we show using first-principles calculations of spin dynamics that the impact of electric fields and substrates on spin-phonon relaxation resolve both discrepancies mentioned above. First, the spin-phonon relaxation time drops by two orders of magnitude due to these effects, matching the typical measured spin lifetimes at the nanosecond scale at room temperature. Second, explicitly including a hexagonal boron nitride (hBN) substrate in the first-principles calculation results in a

non-trivial modification of the SO field, and leads to predicted anisotropy of spin relaxation times that greatly exceed 1/2, also in agreement with experiment.

We start with the simpler analysis of the SO field in first principles calculations compared to previous models, before presenting first-principles calculations of spin-phonon relaxation. Conventionally, theoretical studies approximate the impact of the substrate-induced SO field as a Bychkov-Rashba term in the effective Hamiltonian, containing an undetermined SO coupling-strength parameter.^{12,13,17,21} In the simplest case, the substrate-induced SO field modification is assumed to behave like an electric field applied perpendicular to the graphene plane.¹² This results in a fully in-plane effective SO magnetic field, $\mathbf{B}_{\mathbf{k}}$, which is constant in magnitude but varies in direction with wave-vector \mathbf{k} . However, realistic substrates can create an atomic-scale electrostatic potential variation on the graphene that is much more complex than a uniform electric field. Correspondingly, the directionality of the substrate SO field may differ strongly from the simple picture above.

We find that first-principles calculations indeed show qualitative differences in the direction and magnitudes of the SO field between free-standing graphene with an applied electric field compared to graphene on an hBN substrate (FIG. 1). We select hBN as the prototypical substrate for graphene, known to exhibit reduced extrinsic scattering due to low trapped charge densities and a flat profile,²² and for which several high-quality spin lifetime measurements are available.^{9,15,23} Figure 1 specifically shows the internal SO magnetic field $\mathbf{B}_{\mathbf{k}}$ for doped material with a Fermi level position $\varepsilon_F = 0.1$ eV above the conduction band edge, extracted for each point on the Fermi circle from the spin-orbit energy split $\Delta E_{\mathbf{k}} = g_e \mu_B \mathbf{B}_{\mathbf{k}} \cdot \langle \mathbf{S} \rangle_{\mathbf{k}}$. Here, $\langle \mathbf{S} \rangle_{\mathbf{k}}$ is the spin expectation value for one of the SO-split bands, and $g_e \mu_B$ is the electron spin gyromagnetic ratio.

Free-standing graphene with no electric field (FIG. 1(a)) is inversion symmetric and Kramers degenerate, leading to $\mathbf{B}_{\mathbf{k}} = 0$. In this case, spin-orbit coupling only introduces a small band gap ~ 0.02 meV, as is well-known.²⁴ Applying a transverse electric field to free-standing graphene (FIG. 1(b)) breaks the inversion symmetry, splits the conduction and valence

arXiv:2012.11550v1 [cond-mat.mtrl-sci] 21 Dec 2020

* These authors contributed equally

† yuanping@ucsc.edu

‡ sundar@rpi.edu

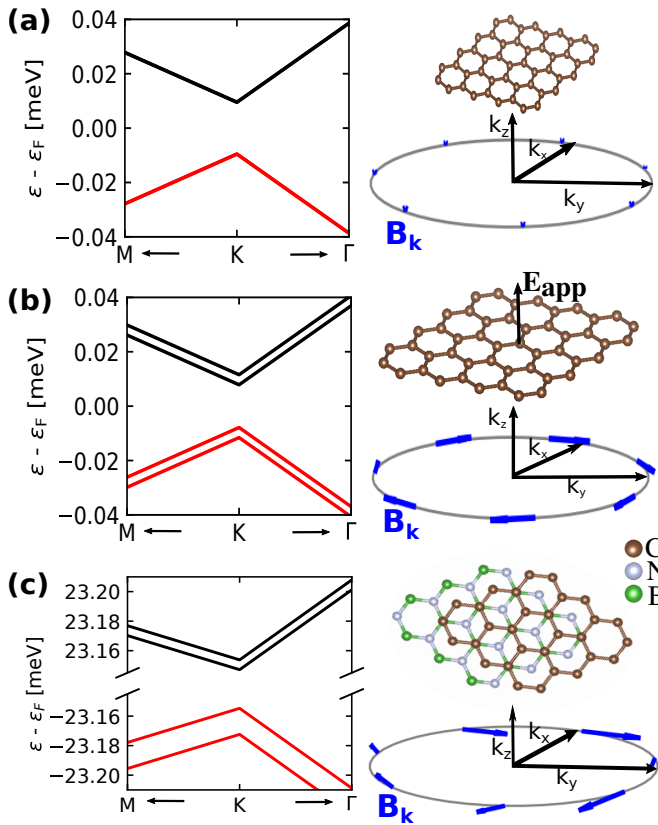


FIG. 1. Band structure in the vicinity of the K point (left panels) and corresponding k -dependent effective SO magnetic field $\mathbf{B}_{\mathbf{k}}$ at a Fermi circle 0.1 eV above the conduction band edge (right panels) for (a) free-standing graphene, (b) graphene with electric field, $E_z = 0.4$ eV/nm, and (c) graphene on hBN. The effect of hBN differs qualitatively from that of an electric field, splitting the valence band stronger than the conduction band and introducing an out-of-plane component to $\mathbf{B}_{\mathbf{k}}$.

bands symmetrically and introduces an in-plane azimuthal magnetic field.¹² Finally, for graphene on hBN (FIG. 1(c)), the valence band splitting is much stronger than that for the conduction band, a larger overall band gap of 46 meV opens up. Most importantly, the SO field $\mathbf{B}_{\mathbf{k}}$ is no longer in-plane, and picks up a significant out-of-plane component from the substrate interaction.

The direction of the effective internal magnetic field directly impacts the anisotropy ratio in the spin lifetimes. Within the D'yakov-Perel (DP) relaxation mechanism,²⁵ often assumed for spin-phonon relaxation in inversion-symmetry-broken systems, the spin relaxation rate is proportional to the rate of spin precession and the momentum relaxation time. Since spin precession is caused by the internal magnetic field perpendicular to the spin direction, this leads to $(\tau_s^i)^{-1} \propto \tau_p (\langle |\mathbf{B}_{\mathbf{k}}|^2 \rangle - \langle (B_{\mathbf{k}}^i)^2 \rangle)$, where $i = x, y, z$ are Cartesian directions, τ_p is the momentum relaxation time and $\langle \rangle$ indicates averaging over \mathbf{k} (i.e. over the Fermi circle here).¹² Consequently, a purely in-plane $\mathbf{B}_{\mathbf{k}}$, as is the case for free-standing graphene with an electric field (FIG. 1(b)), leads to $\tau_s^x = \tau_s^y = 2\tau_s^z$, or $\tau_{s\perp}/\tau_{s\parallel} = 1/2$, assuming symme-

try between the in-plane (\parallel) directions. In contrast, an out-of-plane component to $\mathbf{B}_{\mathbf{k}}$, as present for graphene on hBN (FIG. 1(c)), leads to $\tau_{s\perp}/\tau_{s\parallel} > 1/2$.

Figure 2(a) compares predictions of $\tau_{s\perp}/\tau_{s\parallel}$ from the internal magnetic field using the DP formula above, with explicit first-principles simulations of spin-phonon relaxation (as detailed below). Note that free-standing graphene, with or without a field, shows a ratio of 1/2 in the first-principles spin-phonon calculations, exactly as expected from the DP formula (not shown). In graphene on hBN, both the DP formula and the first-principles calculations show a ratio exceeding 1/2, varying with carrier density and with the maximum value near the neutral (undoped) case. The simple DP formula applied to a realistic SO field extracted from first-principles calculations captures qualitative trends in the spin anisotropy ratio, but the precise magnitudes and dependence on carrier density differ.

We have so far shown that the impact of the substrate on the electronic structure of graphene has a qualitatively different effect on the spin relaxation anisotropy compared to an applied electric field. Next, we show that first-principles calculations of the spin-phonon scattering also reveal a dramatically different picture of substrate effects on spin-phonon relaxation, compared to previous model studies. Previous theoretical estimates of spin-phonon relaxation in graphene employ approximate models of the phonon dispersion and electron-phonon interactions; these models find insignificant changes to the overall spin-phonon relaxation times due to substrates.^{12,13,17} With predicted spin-phonon relaxation times remaining in the order of microseconds, rather than nanoseconds as observed in experiment, the measured relaxation times have previously been attributed to other relaxation mechanisms. However, we now find that a fully first-principles treatment of spin-phonon relaxation reduces the relaxation time to the order of nanoseconds in remarkable agreement with experiments, suggesting that spin-phonon relaxation is in fact the dominant mechanism at room temperature.

To predict spin-phonon relaxation dynamics from first principles, we employ *ab initio* density-matrix dynamics simulations in a Lindbladian formalism, which we recently showed to accurately predict spin relaxation times in a wide variety of materials with varying electronic structure and symmetry.²⁶ Briefly, tracing out the phonon degrees of freedom from the quantum Liouville equation of the combined electron-phonon system and applying the Born-Markov approximation²⁷ leads to the Lindbladian dynamics,²⁸

$$\frac{\partial \rho_{\alpha_1 \alpha_2}}{\partial t} = \frac{2\pi}{\hbar N_q} \sum_{q\lambda \pm \alpha' \alpha'_2} n_{q\lambda}^{\pm} \times \text{Re} \left[\begin{array}{l} (I - \rho)_{\alpha_1 \alpha'} A_{\alpha' \alpha'_1}^{q\lambda \pm} \rho_{\alpha'_1 \alpha'_2} A_{\alpha'_2 \alpha_2}^{q\lambda \mp} \\ - A_{\alpha_1 \alpha'}^{q\lambda \mp} (I - \rho)_{\alpha' \alpha'_1} A_{\alpha'_1 \alpha'_2}^{q\lambda \pm} \rho_{\alpha'_2 \alpha_2} \end{array} \right]. \quad (1)$$

Here, each α denotes an electron wave-vector k and band index n combination, \pm labels absorption and emission of phonons of wave vector $q = \mp(k - k')$ and mode in-

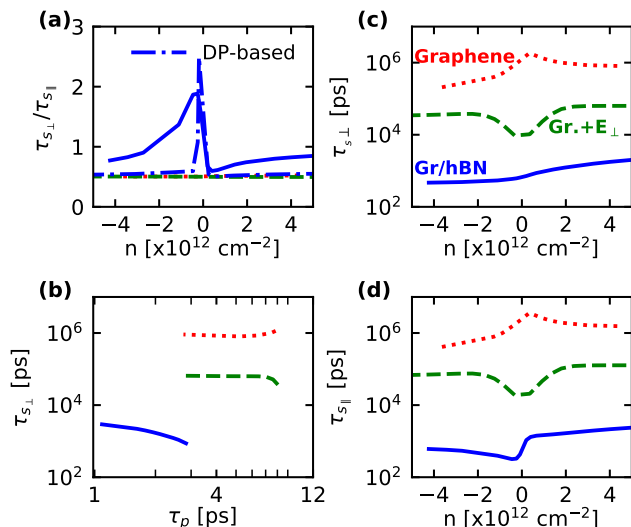


FIG. 2. First-principles spin-phonon relaxation times (τ_s) in graphene, graphene with 0.4 eV/nm electric field and graphene on hBN, as a function of carrier density at room temperature. (a) The out-of-plane to in-plane ratio deviates dramatically from 1/2 for the hBN substrate, partially captured by the DP formula due to the out-of-plane SO field (FIG. 1(b)). (b) Spin lifetime is appreciably inversely correlated with momentum lifetime (τ_p), as expected in the DP mechanism, only for graphene on hBN. Most importantly, both the (c) in-plane and (d) out-of-plane spin lifetime dramatically reduce due to inversion symmetry breaking by either electric field or hBN substrate, with the dependence on carrier density flipped relative to the free-standing case.

index λ , and $n_{q\lambda}^{\pm} \equiv n_{q\lambda} + 0.5 \pm 0.5$ where $n_{q\lambda}$ is the Bose occupation factor of phonon with frequency $\omega_{q\lambda}$. Above, $A_{\alpha\alpha'}^{q\lambda\pm} = g_{\alpha\alpha'}^{q\lambda\pm} \delta^{1/2}(\varepsilon_{\alpha} - \varepsilon_{\alpha'} \pm \hbar\omega_{q\lambda}) \exp(it(\varepsilon_{\alpha} - \varepsilon_{\alpha'}))$ is the electron-phonon matrix element ($g_{\alpha\alpha'}^{q\lambda\pm}$) along with time dependence in the interaction picture and energy conservation, where ε_{α} are the electron energies. All electron and phonon energies and matrix elements are calculated on coarse k and q meshes in the plane-wave density-functional theory software, JDFTx,²⁹ and are then interpolated to extremely fine meshes in a basis of maximally localized Wannier functions.^{30–33} We evolve Eq. (1) in time using an adaptive Runge-Kutta integrator starting from both in-plane and out-of-plane spin-polarized states, compute the spin expectation values $\text{Tr}[\mathbf{S}\rho(t)]$ for each, and thereby extract the spin relaxation times $\tau_{s\parallel}$ and $\tau_{s\perp}$. See Refs. 26 and 34 for further details on the formalism and the supplemental material for computational details.³⁵

Figure 2 shows our first-principles calculations of spin-phonon relaxation in graphene with and without electric field, and graphene on hBN, each as a function of carrier density (doping). As discussed already above, the ratio $\tau_{s\perp}/\tau_{s\parallel}$ deviates substantially from 1/2 only for graphene on hBN (FIG. 2(a)), and the simple DP formula estimate based on the SO field direction only captures part of this dramatic effect seen in our first-principles calculations and experiment. The D'yakonov

Perel (DP) mechanism²⁵ is the predominant simplified picture of spin-phonon relaxation in inversion-symmetry-broken systems, in contrast to the Elliott-Yafet (EY) mechanism^{36,37} for inversion-symmetric systems. Briefly, in the EY case, SO-based spin mixing facilitates spin-flip transitions between pairs of Kramers degenerate states, leading to a direct correlation between spin-phonon and other electron-phonon relaxation processes, such as $\tau_s \propto \tau_p$, the momentum relaxation time. In contrast, the DP mechanism involves electron spins precessing between scattering events due to the internal SO magnetic field, resulting in $\tau_s \propto \tau_p^{-1}$. Our first-principles calculations in FIG. 2(b) show a weak positive correlation between τ_s and τ_p in inversion-symmetric free-standing graphene, which switches to a weak negative correlation when inversion symmetry is broken with an applied electric field, and a stronger negative correlation when that symmetry is broken by an hBN substrate. This qualitatively matches the switch from EY to DP mechanism upon inversion symmetry breaking,^{5,14,18,23,38} but neither simplified mechanism explains the trends in the first-principles predictions quantitatively.

Importantly, in this first-principles study, we predict spin-phonon relaxation without assuming any of the above special cases and without any empirical parameters in the electronic structure, phonon dispersion or electron-phonon coupling. Figures 2(c) and (d) respectively show the out-of-plane ($\tau_{s\perp}$) and in-plane ($\tau_{s\parallel}$) spin relaxation lifetimes as a function carrier density. Inversion symmetry breaking by a transverse electric field of 0.4 eV/nm reduces the lifetimes by two orders of magnitude at low carrier densities and one order of magnitude at carrier densities exceeding 10^{12} cm^{-2} , with resulting lifetimes in tens of nanoseconds. The hBN substrate reduces lifetimes further, down to a few nanoseconds, exactly as measured in experiments.^{5,8,9,15} Critically, we find these reduced lifetimes purely due to modifications of the spin-orbit fields, phonon dispersion and electron-phonon coupling due to the substrate; we did not need to account for defects or disorder to match the measured scale of spin relaxation times.^{12,13,17–20}

The spin lifetime depends on carrier density in all cases (FIG. 2(c,d)), and is almost symmetric between electrons and holes for free-standing graphene with or without electric fields. However, the substrate substantially breaks electron-hole symmetry, with hole lifetimes 2-3x smaller than electron lifetimes, in agreement with experimental measurements on hBN and SiO₂ substrates.^{4,5,9,10,38} This asymmetry derives from the larger SO splitting (internal magnetic field) for the valence band compared to the conduction band, as shown in FIG. 1(c). Further, the spin lifetime decreases with increasing magnitude of carrier density in inversion-symmetric graphene, but this trend reverses and spin lifetime increases with carrier density magnitude for both inversion-symmetry-broken cases, once again in agreement with experiment.^{5,9}

So far, we have seen that the hBN substrate has a stronger and electron-hole asymmetric impact on spin-phonon relaxation in graphene, compared to an applied electric field. Next, we consider the impact of electric

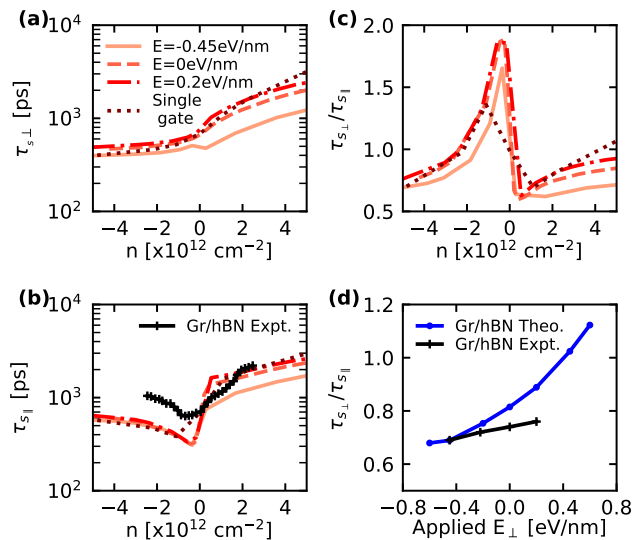


FIG. 3. (a) Out-of-plane and (b) in-plane spin-phonon relaxation times in graphene on hBN can be further tuned by an applied electric field. (Experimental data from Ref. 8.) With a single gate, the electric field is dependent on the carrier density and cannot be varied independently. Variation of $\tau_{s\perp}/\tau_{s\parallel}$ ratio with (c) carrier density at specified electric fields, and with (d) electric field at a carrier density of $3.7 \times 10^{12} \text{ cm}^{-2}$, showing strong deviations from 1/2 in agreement with experiment.¹⁵

fields on graphene on hBN. Experimentally, this is best achieved with a top and bottom gate so that the combination of two biases can be used to control the net electric field and carrier density in the graphene independently.¹⁵ In contrast, a single gate constrains the electric field and carrier density to vary co-dependently as $E = en/(2\epsilon_0)$ by Gauss's law. We consider both cases – dependent and independent control of electric field and carrier density – in FIG. 3. As discussed above, the spin lifetimes are larger for electrons than holes: positive electric fields serve to enhance this asymmetry, while negative electric fields reduce it. The predicted in-plane spin lifetimes (FIG. 3(b)) agree well with measurements from Ref. 8 which employs a single gate, but slightly overestimate the electron-hole asymmetry in comparison.

Applied electric fields on graphene on hBN also modify the ratio between out-of-plane and in-plane spin lifetimes, increasing it for holes and reducing for electrons as shown in FIG. 3(c). We also compare the predicted ratio directly with experimental measurements¹⁵ at the same electron density of $3.7 \times 10^{12} \text{ cm}^{-2}$ in FIG. 3(d). We find excellent agreement for negative applied fields, but slightly overestimate the increase of ratio with electric field. The remaining discrepancy with experiments in FIG. 3(b) and (d) can be attributed to additional scattering, such as due to defects and impurities. Note that in the inversion-symmetry broken case, additional scattering serves to reduce the momentum relaxation time τ_p , which is expected to increase the overall spin lifetimes and bring the ratio closer to 1/2 according to the DP model.¹² We re-emphasize that our first-principles calculations show

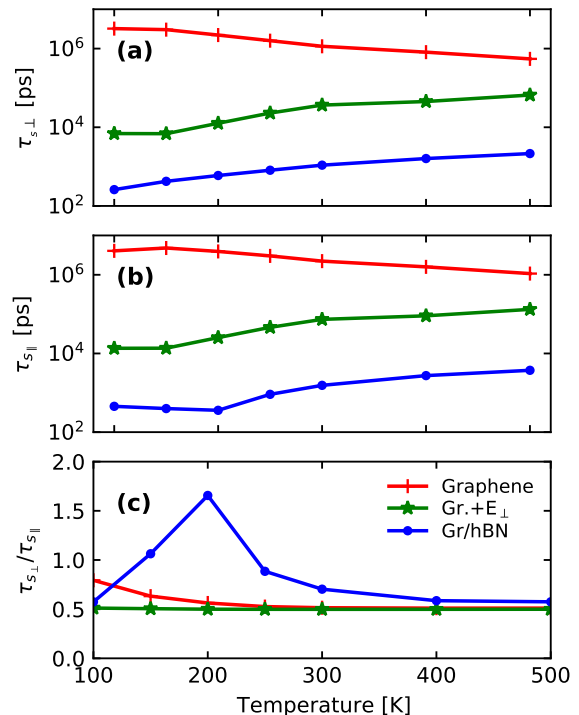


FIG. 4. (a) Out-of-plane and (b) in-plane spin-phonon lifetimes predominantly decrease with increasing temperature in graphene, but increase with increasing temperature when inversion symmetry is broken by electric fields or an hBN substrate (shown for Fermi level $\sim 0.1 \text{ eV}$ above conduction band minimum or electron density $\approx 1 \times 10^{12} \text{ cm}^{-2}$). (c) The corresponding ratio is pinned to 1/2 for graphene with electric field, but deviates from 1/2 at lower temperatures, weakly for free-standing graphene and strongly for graphene on hBN.

that spin-phonon relaxation captures the typical magnitudes and trends in agreement with experiment, requiring only minor modifications due to additional scattering, in contrast with previous models that predicted spin-phonon relaxation times several orders of magnitude greater than in experiment.

Finally, we investigate the temperature dependence of spin-phonon relaxation in graphene-based devices. Previous theoretical studies predict weak temperature dependence for graphene on a substrate,¹² compared to an inverse relation between temperature and spin lifetimes in free-standing graphene.¹³ Our first-principles calculations show that the spin lifetimes indeed decrease with increasing temperature for free-standing graphene due to increased phonon scattering (FIG. 4(a,b)). However, inversion symmetry broken by either field or substrate, we predict the opposite trend of lifetime increasing with increasing temperature in agreement with experiments.^{4,38} Figure 4(c) further reveals that the anisotropy ratio is pinned to 1/2 for graphene with electric fields, as expected for the DP mechanism, and the deviation from 1/2 for graphene on hBN increase at lower temperatures where the substrate SO field has a larger influence.

In conclusion, using first-principles predictions based on Lindbladian density-matrix dynamics, we have shown

that spin-phonon relaxation in graphene is at least two orders of magnitude stronger than previously believed due to the critical impact of electric fields and substrate interactions. This resolves the long-standing mystery of measured spin lifetimes in graphene being much smaller than theoretical predictions. Additionally, we find that substrate modifications to the spin-orbit field and phonon interactions increase the ratio between out-of-plane and in-plane spin lifetimes from 1/2 based on previous theoretical predictions to values exceeding 0.7 in agreement with experiment. These two independent pieces of ev-

idence strongly suggest that spin-phonon relaxation accounting for substrate phonons and electronic structure modifications is the primary mechanism for spin relaxation in graphene at room temperature.

Acknowledgements: This work is supported by National Science Foundation under grant No. DMR-1956015. AH acknowledges support from the American Association of University Women (AAUW) fellowship program. Calculations were carried out at the Center for Computational Innovations at Rensselaer Polytechnic Institute.

-
- [1] A. K. Geim and K. S. Novoselov, *Nature Materials* **6**, 182 (2007).
- [2] P. Recher and B. Trauzettel, *Nanotechnology* **21**, 302001 (2010).
- [3] W. Han, M. Gmitra, and J. Fabian, *Nature Nanotechnology* **9**, 794 (2014).
- [4] W. Han and R. K. Kawakami, *Phys. Rev. Lett.* **107**, 047207 (2011).
- [5] P. J. Zomer, M. H. D. Guimarães, N. Tombros, and B. J. van Wees, *Phys. Rev. B* **86**, 161416 (2012).
- [6] W. Han, J.-R. Chen, D. Wang, K. M. McCreary, H. Wen, A. G. Swartz, J. Shi, and R. K. Kawakami, *Nano Letters* **12**, 3443 (2012).
- [7] M. B. Lundberg, R. Yang, J. Renard, and J. A. Folk, *Phys. Rev. Lett.* **110**, 156601 (2013).
- [8] M. Drögeler, F. Volmer, M. Wolter, B. Terrés, K. Watanabe, T. Taniguchi, G. Güntherodt, C. Stampfer, and B. Beschoten, *Nano Letters* **14**, 6050 (2014).
- [9] M. Drögeler, C. Franzen, F. Volmer, T. Pohlmann, L. Banszerus, M. Wolter, K. Watanabe, T. Taniguchi, C. Stampfer, and B. Beschoten, *Nano Letters* **16**, 3533 (2016).
- [10] B. Raes, J. E. Scheerder, M. V. Costache, F. Bonell, J. F. Sierra, J. Cuppens, J. Van de Vondel, and S. O. Valenzuela, *Nature Communications* **7**, 11444 (2016).
- [11] S. Ringer, S. Hartl, M. Rosenauer, T. Völkl, M. Kadur, F. Hopperditzel, D. Weiss, and J. Eroms, *Phys. Rev. B* **97**, 205439 (2018).
- [12] C. Ertler, S. Konschuh, M. Gmitra, and J. Fabian, *Phys. Rev. B* **80**, 041405 (2009).
- [13] I. M. Vicent, H. Ochoa, and F. Guinea, *Phys. Rev. B* **95**, 195402 (2017).
- [14] N. Tombros, S. Tanabe, A. Veligura, C. Jozsa, M. Popinciuc, H. T. Jonkman, and B. J. van Wees, *Phys. Rev. Lett.* **101**, 046601 (2008).
- [15] M. H. D. Guimarães, P. J. Zomer, J. Ingla-Aynés, J. C. Brant, N. Tombros, and B. J. van Wees, *Phys. Rev. Lett.* **113**, 086602 (2014).
- [16] A. Avsar, H. Ochoa, F. Guinea, B. Özyilmaz, B. J. van Wees, and I. J. Vera-Marun, *Rev. Mod. Phys.* **92**, 021003 (2020).
- [17] S. Fratini, D. Gosálbez-Martínez, P. Merodio Cámara, and J. Fernández-Rossier, *Phys. Rev. B* **88**, 115426 (2013).
- [18] D. Van Tuan, F. Ortmann, D. Cummings, Aron W. and Soriano, and S. Roche, *Scientific Reports* **6**, 21046 (2016).
- [19] D. Van Tuan, F. Ortmann, D. Soriano, S. O. Valenzuela, and S. Roche, *Nature physics* **10**, 857 (2014).
- [20] D. Kochan, M. Gmitra, and J. Fabian, *Phys. Rev. Lett.* **112**, 116602 (2014).
- [21] K. Zollner, M. Gmitra, and J. Fabian, *Phys. Rev. B* **99**, 125151 (2019).
- [22] C. R. Dean, A. F. Young, I. Meric, C. Lee, L. Wang, S. Sorgenfrei, K. Watanabe, T. Taniguchi, P. Kim, K. L. Shepard, and J. Hone, *Nature Nanotechnology* **5**, 722 (2010).
- [23] M. Gurrum, S. Omer, and W. B. J. van, *2D Materials* **5**, 032004 (2018).
- [24] S. Konschuh, M. Gmitra, and J. Fabian, *Phys. Rev. B* **82**, 245412 (2010).
- [25] M. Dyakonov and V. Perel, *Soviet Physics Solid State, USSR* **13**, 3023 (1972).
- [26] J. Xu, A. Habib, S. Kumar, F. Wu, R. Sundararaman, and Y. Ping, *Nature Communications* **11**, 2780 (2020).
- [27] D. Taj, R. Iotti, and F. Rossi, *Eur. Phys. J. B* **72**, 305 (2009).
- [28] R. Rosati, F. Dolcini, and F. Rossi, *Phys. Rev. B* **92**, 235423 (2015).
- [29] R. Sundararaman, K. Letchworth-Weaver, K. A. Schwarz, D. Gunceler, Y. Ozhabes, and T. Arias, *SoftwareX* **6**, 278 (2017).
- [30] N. Marzari and D. Vanderbilt, *Phys. Rev. B* **56**, 12847 (1997).
- [31] A. M. Brown, R. Sundararaman, P. Narang, W. A. Goddard, and H. A. Atwater, *ACS Nano* **10**, 957 (2016).
- [32] P. Narang, L. Zhao, S. Claybrook, and R. Sundararaman, *Adv. Opt. Mater.* **5**, 1600914 (2017).
- [33] A. Habib, R. Florio, and R. Sundararaman, *J. Opt.* **20**, 064001 (2018).
- [34] J. Xu, A. Habib, R. Sundararaman, and Y. Ping, “*Ab initio* ultrafast spin dynamics in solids,” (2020), preprint: arXiv:2012.08711.
- [35] See attached supplemental information [URL inserted by publisher] for computational details.
- [36] R. Elliott, *Phys. Rev.* **96**, 266 (1954).
- [37] Y. Yafet, in *Solid State Phys.*, Vol. 14 (Elsevier, 1963) pp. 1–98.
- [38] A. Avsar, T.-Y. Yang, S. Bae, J. Balakrishnan, F. Volmer, M. Jaiswal, Z. Yi, S. R. Ali, G. Güntherodt, B. H. Hong, B. Beschoten, and B. Özyilmaz, *Nano Letters* **11**, 2363 (2011).